Available online at www.sciencedirect.com
SCIENCE DIRECT®
Biochemical and Biophysical Research Communications 334 (2005) 569–576
BBRC
www.elsevier.com/locate/ybbrc

Cloning and expression of Ca^{2+}-activated chloride channel from rat brain

Sang Min Jeong [a], Hye-Kyung Park [b], In-Soo Yoon [a], Jun-Ho Lee [a], Jong-Hoon Kim [a], Choon-Gon Jang [c], C. Justin Lee [b], Seung-Yeol Nah [a,*]

[a] Department of Physiology, College of Veterinary Medicine, Konkuk University, Seoul 143-701, Republic of Korea
[b] Korea Institute of Science and Technology, Seoul 136-791, Republic of Korea
[c] Department of Pharmacology, College of Pharmacy, Sungkyunkwan University, Suwon 440-746, Republic of Korea

Received 27 May 2005
Available online 1 July 2005

Abstract

To clone the gene product responsible for the calcium-activated chloride channel (CLCA) in rat brain cerebrum, we performed a reverse transcription-PCR (RT-PCR) with gene-specific primers of a rat EST clone. We successfully cloned a rat brain CLCA (rbCLCA). The full-length cDNA is 2895 bp long and codes for a 902 amino acid protein. The clone consists of four transmembrane domains and shows a 79.1% of significant homology with previously reported mouse smooth muscle chloride channel sequence. We also performed RT-PCR using single neuron and glia, and various tissues to determine the tissue expression of rbCLCA. We found that rbCLCA was expressed in both neuron and glia. In peripheral organs, rbCLCA showed the predominant expressions in cerebrum, cerebellum, kidney, small intestine, and stomach but not in heart, large intestine, liver, lung, and spleen. Whole-cell patch clamp studies in HEK293 cells transfected with the clone identified a niflumic acid (a CLCA channel blocker)-sensitive and voltage-dependent chloride current but we could not observe this chloride current in mock-transfected cells. The identification of genes belonging to the CLCA family from rat brain and its functional expression will help to evaluate its physiological role in brain as anion channel.

Keywords: Ca^{2+}; Chloride channel; Ca^{2+}-activated chloride channel; Neuron; Glia; Central nervous system

Calcium-activated chloride channels (CLCA) have been expressed in a variety of cell types including cardiac muscle [1,2], epithelium [3], neurons and glia [4,5], smooth muscle [6,7], exocrine gland cells [8], and *Xenopus* oocytes [9]. These channels play important physiological roles, including smooth muscle tone, transepithelial fluid secretion, regulations of cell volume, cardiac and neuronal action potential, and a fast blocking of polyspermy [9]. In addition, CLCAs may also be involved in respiratory diseases such as asthma and cystic fibrosis and tumorigenesis. In case of cystic fibrosis, the gene coding cystic fibrosis transmembrane conductance regulator (CFTR) is mutated. This mutation causes a loss of CFTR protein function from plasma membrane of affected cells and results in dysfunction of a cyclic-AMP-regulated, linear and small conductance chloride channel [10–12]. Some CLCA subtypes also are involved in tumor suppressing action or promotes tumor cell apoptosis, since in breast cancer cell lines or colorectal carcinoma cells some of CLCA isoforms are deficient or down-regulated [13–15].

We performed the present study to clone the gene product responsible for the calcium-activated chloride (CLCA) current in rat brain cortex. As noted above, the diverse physiological or pathological roles of these channels in a number of cells or organs (i.e., digestive tracts, eye, lung, mammary gland, smooth muscle, and

* Corresponding author. Fax: +82 2 450 3037.
E-mail address: synah@konkuk.ac.kr (S.-Y. Nah).

0006-291X/$ - see front matter © 2005 Elsevier Inc. All rights reserved.
doi:10.1016/j.bbrc.2005.06.122

trachea) have been reported [16–21] but the molecular identity of CLCA originated from rat brain remains relatively unknown. Moreover, although CLCA currents are observed in neurons and glial cells [4,5], most of CLCA were cloned from non-nervous systems. Here, we report the cloning and functional expression of rat brain CLCA. Like other CLCA genes, rat brain CLCA (rbCLCA) shows a large homology with mCLCA4 [18] and we found that rbCLCA was expressed in both neuron and glia. Transient transfection of HEK293 cells with rbCLCA results in the expression of calcium-activated currents similar to those observed in other CLCAs. These results suggest that rbCLCA is the gene that encodes calcium-activated chloride channels in rat cortex neurons and broadens the physiological and pathological relevancy of the CLCA gene family.

Materials and methods

Materials. Molecular reagents were ordered from iNtRON Biotechnology (Seongnam, Korea), Invitrogen (San Diego, CA), Qiagen (Valencia, CA), Amersham Biosciences (Buckinghamshire, England), BD Science (Franklin Lakes, NJ), Toyobo (Osaka, Japan), Novagen (Madison, WI), or Stratagene (La Jolla, CA), as indicated. pGEM-T Easy and pcDNA 3.1^{+} vector are purchased from Promega (Madison, WI). All other reagents were purchased from Sigma (St. Louis, MO).

EST screening, sequencing, and analysis. A homology search on the EST database was performed with the BLAST Server using mouse CLCAs as the query sequence. The EST containing the rat cornea DNA sequence, which is identified by this search, was obtained from the rat brain. The resulting PCR products were subcloned into pGEM-T Easy vector for sequencing and into pcDNA3.1 for data recording analysis. The routine purification of plasmids for molecular work was prepared by DNA purification kit (DNA-spin, iNtRON Biotechnology).

RNA preparation. Total RNA of various rat tissues was extracted with Trizol (Invitrogen) or easy-BLUE reagents (iNtRON Biotechnology, Korea), using the supplier's manual with some modifications. To avoid any contamination of genomic DNA, the extracted total RNA was digested with RNase-free DNase I (Invitrogen).

Full-length amplification and cDNA cloning. As first step, database was screened with the sequence of mouse calcium-activated chloride channel (mCLCA family) gene sequence. Several sets of gene-specific primers based on the rat EST sequence were designed. In order to obtain the first stranded cDNA, 10 μg each of rat brain RNA was reverse transcribed with reverse transcriptase (Superscript III, Invitrogen) and either gene-specific primers for 5′-RACE or an oligo(dT) primer for 3′-RACE, respectively. 3′ terminal half of cDNA and several rounds of RT-PCR procedure are shown in Fig. 1. The following reaction of 5′-RACE (rapid amplification of cDNA ends) for full-length of cDNA was performed as follows: the concatemerized cDNA with T4 RNA ligase in the presence of 1 mM hexamine cobalt chloride and 25% polyethylene glycol 6000, second strand DNA synthesis was carried out by PCR with primers RC4 and RC5 in KOD-Plus *Taq* polymerase system (Toyobo). Nested PCR was performed with the primers RC6 and RC7. More 5′-RACE reaction was performed using RC12, RC13, RC14, and RC15 primers mentioned

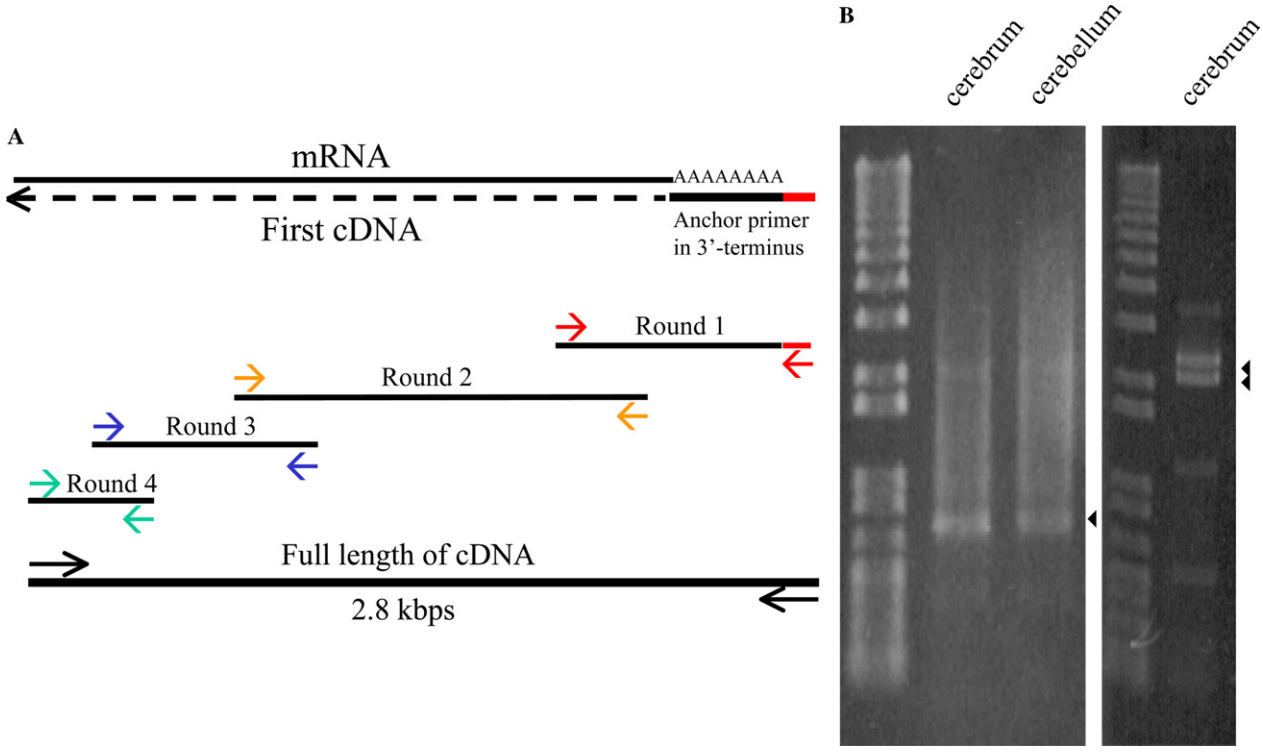

Fig. 1. The construction strategy of full-length cDNA. (A) To obtain the full-length of rbCLCA cDNA, four rounds of PCR are carried out in appropriate conditions. First cDNA (dotted) and PCR products (thick) are depicted with black lines. 3′-RACE products are represented round 1, the 5′-RACE products are also represented round 2, 3, and 4, respectively. (B) PCR products of 3′-RACE (left, round 1) and 5′-RACE (right, round 2) were electrophoresed in a 1% of agarose gel. Black arrowheads indicate the 0.55, 2.2, and 2.4 kbp of target products. Because same products appeared in both the brain tissues, the following 5′-RACE reactions were proceeded with only cerebrum tissues.

Table 1
Primer sequence of rbCLCA for PCR

Primer name	Sequence
RC1	5′-ACCTGGCTACGTTGAAAATGATCAAAT-3′
RC2	5′-AAGCTGCAGTGGAAGACTTCAGCAGAC-3′
RC3	5′-AGACCTCAGAGGTGAGACCGGCT-3′
RC4	5′-GAAACGTTTAAATTCAAACCAGCAAG-3′
RC5	5′-TCTTTAGGTATCAGACCGGAAGTATTCAC-3′
RC6	5′-CAGATCTACATTGCAATTCAGGCCGA-3′
RC7	5′-AAAATCTTGGAGACCAGGAGGATGCC-3′
RC12	5′-TGGGGACAGAGGACGGTAC-3′
RC13	5′-GAAGGGTGTAGGGATTGTCTCC-3′
RC14	5′-CATTTCACTCCAAACTTCCTGCTCAC-3′
RC15	5′-TGAGAATTGGCAACTATGACATCTGC-3′
RC23	5′-GAATGAAATGTATGTACCGTCCTCTG-3′
RC25	5′-GTCGGTAGAACACCTTGTCACTTC-3′
RC29	5′-ACACCATAGCATGTGCGAGC-3′
RC40	5′-agatcaattcccggggatccACACCATAGCATGTGCGAGC-3′
RC41	5′-atgcatatcgatcaattgaattcTTAAAATATGAATAAAGTTGCAAC-3′
RC42	5′-ACTGTCAAACAGGGTACAGGC-3′
RC43	5′-TGTTACCCAGATTAGGGTTGCTGGG-3′
HRMbA1	5′-ATGCCATCCTGCGTCTGGACCTG-3′
HRMbA2	5′-GCGCTCAGGAGGAGCAATGATCTTG-3′
HRMbA3	5′-TCACCCACACTGTGCCCATC-3′
HRMbA4	5′-CTTGCTGATCCACATCTGCTG-3′

in Table 1. Each 25 repeats of 1st PCR consisted of 94 °C for 40 s, 55–56 °C for 40 s, and 68 °C for 3 min 30 s, and 25 repeats of nested PCR conditions were 94 °C for 40 s, 58–60 °C for 40 s, and 68 °C for 3 min 30 s (Fig. 1B). The nested PCR products of three rounds were poly(A) tailed and then inserted into TA cloning vector, pGEM-T Easy (Promega). The full-length of cDNA was completed after several rounds of recombinant PCR using the amplified cDNAs as templates (Fig. 1A). The nucleotide sequences of each step were determined by ABI PRISM system (model 377). First PCR was proceeded with primer RC4 and RC5 for round 2, with primer RC12 and RC13 for round 3, and with primer RC29 and RC23 for round 4. Nested PCR was proceeded with primer RC6 and RC7 for round 2, with primer RC14 and RC15 for round 3, and with primer RC29 and RC23 for round 4 (Table 1).

Reverse transcription-PCR. First, various cDNA derived rat tissues were used for gene-specific amplification. Two rounds of PCR were proceeded using *i*-Star*Taq* polymerase (iNtRON Biotechnology) and gene-specific and internal control primers as in Table 1, independently. First round of PCR was carried out in a Peltier thermal cycler PTC-200 with initial denaturation step at 94 °C for 1 min, followed by 25 repeats of denaturation at 94 °C for 15 s, annealing at 55 °C for 30 s, and elongation at 72 °C for 50 s. The amplified PCR products were purified through S-400 Sephacryl spin column, then one-fiftieth of PCR products were amplified again under the following conditions using nested primers: 94 °C for 1 min, 20 repeats of denaturation at 94 °C for 15 s, annealing at 63 °C for 30 s, and elongation at 72 °C for 40 s.

Slice preparation and the mechanical dissociation. Hippocampal slices were prepared from 5-week-old male rats. Rat brains were quickly cooled in iced artificial cerebrospinal fluid (ACSF, which contained in (mM) 124 NaCl, 2.5 KCl, 2 $CaCl_2$, 2 $MgSO_4$, 1.25 NaH_2PO_4, 26 $NaHCO_3$, and 10 glucose, pH 7.4, after bubbling with mixed 95% O_2–5% CO_2 gas). After cooling for 5 min, the hippocampus was dissected out along with the surrounding cortex and sliced into 400 μm-thick sections with a Leica vibratome LV1000S. Slices were incubated in ACSF buffer supplied with a mixture of 95% O_2 and 5% CO_2 gas mixture for 1 h at room temperature. The hippocampal slices were transferred onto a cover glass coated poly-D-lysine. A heavily fire-polished blunt pipette is horizontally vibrated across the surface of the hippocampus at a frequency of 30 Hz and with an amplitude displacement of 1.0 mm. The treated slice is then removed and the liberated cells are left to settle onto the base of the dish. For picking cells, we used a glass microelectrode filled with ACSF. The single cells were picked under a microscope [22].

Reverse transcription-PCR of single cell. Total RNA of in vivo single cells is extracted with easy-BLUE reagents (iNtRON Biotechnology, Korea) as mentioned in the section of RNA preparation. Total RNA was reverse transcribed with reverse transcriptase (Sensiscript, Qiagen) and either cell specific primers. Three rounds of PCR were proceeded using *i*-Star*Taq* polymerase (iNtRON Biotechnology) and gene-specific and other control primers, independently. Two sets of first round PCR were carried out in a Peltier thermal cycler PTC-200 with initial denaturation step at 94 °C for 1 min, followed by five repeats of denaturation at 94 °C for 10 s, annealing at 62 °C for 30 s, and elongation at 72 °C for 1 min 50 s, and then followed by 15 repeats of denaturation at 94 °C for 10 s, annealing at 60 °C for 30 s, and elongation at 72 °C for 1 min 50 s. The amplified PCR products were purified through the disposable spin column (PROBER, iNtRON), then one-twentieth of PCR products were amplified again by additional two rounds of PCR under the following conditions using nested primers. Two sets of second round PCR were performed with initial denaturation step at 94 °C for 1 min, followed by five repeats of denaturation at 94 °C for 15 s, annealing at 62 °C for 40 s, and elongation at 72 °C for 2 min, and then followed by 30 repeats of denaturation at 94 °C for 15 s, annealing at 60 °C for 40 s, and elongation at 72 °C for 2 min. After the addition of 2.5 U of *i*-Star*Taq* polymerase, two more sets of third round PCR were performed with initial denaturation step at 94 °C for 1 min, followed by five repeats of denaturation at 94 °C for 10 s, annealing at 57 °C for 30 s, and elongation at 72 °C for 50 s, and then followed by 50 repeats of denaturation at 94 °C for 10 s, annealing at 55 °C for 30 s, and elongation at 72 °C for 50 s.

Plasmid construction for the transfection to HEK293 cells. The full-length of cDNA was amplified by KOD-Plus *Taq* polymerase system using the *Bam*HI, *Eco*RI site-attached RC40 and RC41 primers, respectively. Restriction enzyme-digested cDNA was directionally inserted downstream of CMV promoter of pcDNA 3.1^+ vector (Invitrogen). The sequence of completed constructs was confirmed by sequencing. The plasmid for infection to HEK293 cells was prepared by plasmid maxi kit (Qiagen).

Heterologous expression of rbCLCA in HEK293 cells. rbCLCA subcloned in pcDNA3.1 was co-transfected into HEK293 cells with EGFP vector alone or EGFP and pcDNA3.1. Plasmid transfection was carried out with Ca^{2+}–PO_4 precipitation (Clontech). Transfected cells were dissociated and replated 1 day after transfection and spread on glass coverslips. Fluorescent cells were used for patch-clamp experiments within 3 days.

Whole-cell recordings. HEK293 cells were transfected with a rbCLCA expression plasmid mixed with an EGFP plasmid at a 10:1 ratio by using Lipofectamine 2000 (Invitrogen) at 1 μg of DNA per 1.5 cm well plate. The EGFP plasmid alone (100 ng) was used as a transfection control. Approximately, 36 h after transfection, whole-cell recordings were performed on single isolated green cells identified under a fluorescence microscope. Standard extracellular solution contained (in mM): 150 NaCl, 3 KCl, 2 $CaCl_2$, 2 $MgCl_2$, 2 glucose, 2 sucrose, and 10 Hepes, pH 7.4. Standard pipette solution contained (in mM): 146 CsCl, 2 $MgCl_2$, 5 Ca-EGTA-NMDG, 10 sucrose, and 8 Hepes, pH 7.3. Free Ca^{2+} concentration is estimated to be 4.5 μM [16]. Data were acquired with an Axopatch 200A amplifier controlled by Clampex 9.0 via a Digidata 1322A data acquisition system (Axon Instruments, Foster City, CA).

Results and discussion

Since cloning and expression of most CLCAs were performed in human, mouse, and non-nervous systems, we, in present study, have planned to clone rat brain CLCA. We utilized the expressed sequence tags (EST) in sequence database, which gives new genes belonging to a given protein family. For this, we performed a BLAST search using the mouse CLCA subtypes as the query sequence. We found that rat cornea cDNA fragment (R.n EST1) shows a high sequence identity with mouse CLCA subtypes (45–75%, data not shown). Using this partial rat cornea cDNA fragment we cloned full-length coding sequence according to the procedures as mentioned under Materials and methods and determined of the entire 2895 bp of cDNA sequence including an large open reading frame. We also found that

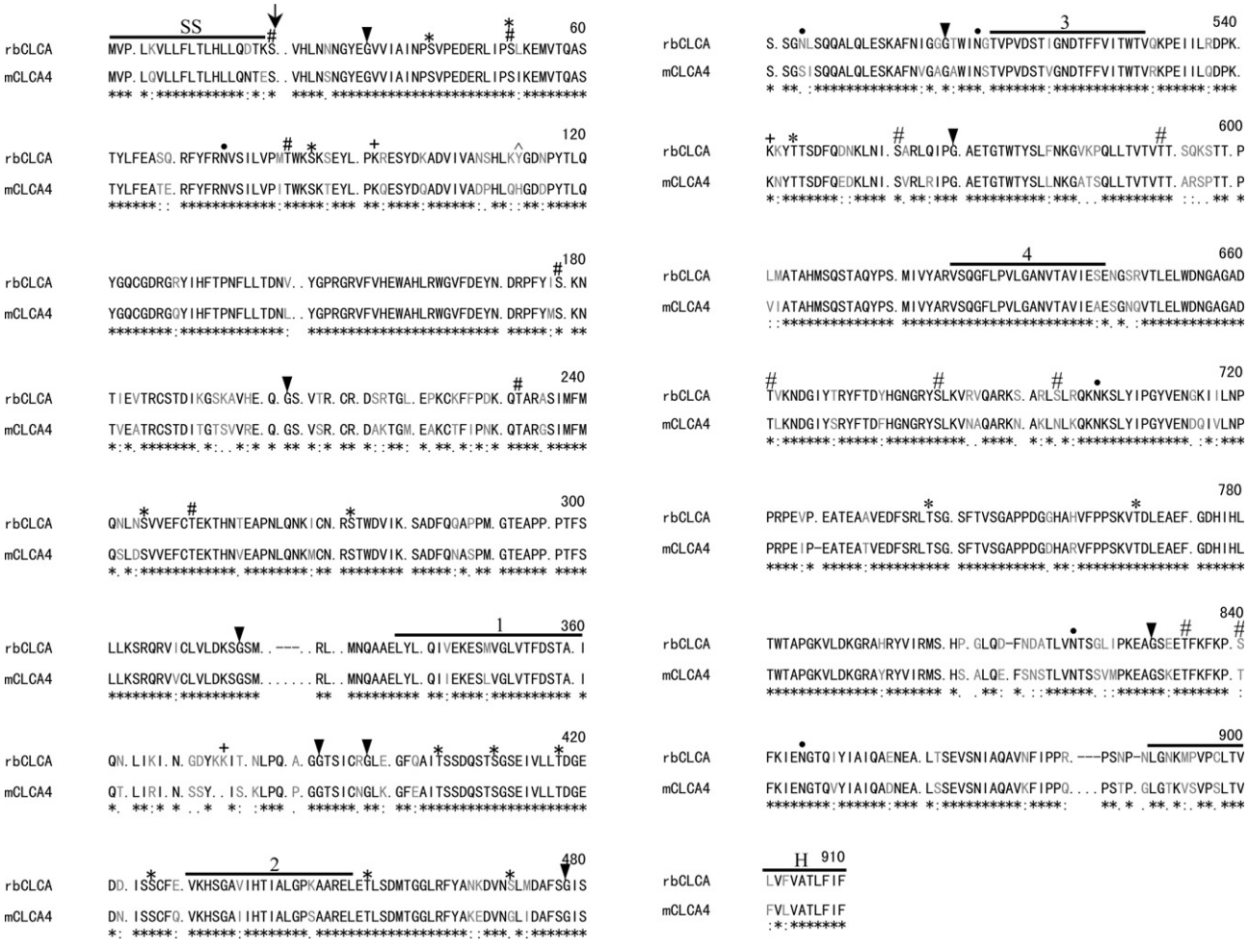

Fig. 2. Comparison of rbCLCA structure. Amino acid alignment was deduced by querying the rbCLCA amino acid sequence with CLUSTAL W methods. The predicted amino acid sequence (top strand) aligned with those of mCLCA4. Identical amino acids are indicated below each column by asterisk. The hydrophobic regions are overlined putative four transmembrane regions and assigned as signal sequence (SS) and hydrophobic carboxyl terminus (H). An arrow indicates the predicted cleavage site. The motif site of N-myristoylation is marked with arrowheads. Consensus sites are marked for N-linked glycosylation (●), for phosphorylation by PKC (#), by cAMP and cGMP-dependent protein kinase (+), by tyrosine kinase (^) and for phosphorylation by casein kinase II (*).

this cDNA comprises a short 5′- and a 3′-untranslated sequence (UTR) followed by a poly(A)$^+$ tail. A polyadenylation signal-like sequence (ATTAAA) was found at bases 16–21 upstream of the poly(A)$^+$ tail. This full-length of cDNA sequence will appear in the GenBank/EMBL/DDBJ nucleotide sequence databases with the Accession No. AB212889.

The protein deduced from the coding sequence has 902 amino acids and is highly homologous to the mouse CLCA1, -2, and -4 [14,18,19]. The open reading frame of rbCLCA shows 82.0%, 83.1%, 49.4%, 79.1%, 45.3%, and 48.4% identity overall to that of mCLCA1, 2, 3, 4, 5, and 6, respectively. Although mCLCA1 and mCLCA2 were most homologous to rbCLCA, they were not identical in their carboxyl terminus except mClCA4 (data not shown). Thus, the amino acid sequence of rbCLCA carboxyl terminus was most significantly homologous to that of mCLCA4 [18]. The entire amino acid sequences of these two proteins are identical by 79.1% are uniformly distributed along the entire sequence (Fig. 2). That rbCLCA also included the sites of signal peptidase cleavage, N-linked glycosylation, phosphorylation by PKC, cAMP- and cGMP-dependent protein kinase, tyrosine kinase, and casein kinase II (Fig. 2). Hydropathy analysis of the full-length rbCLCA open reading frame using an analysis window of 17 residues revealed four major potential transmembrane-spanning domains as well as several minor regions, which is well consistent with a membrane protein (Fig. 3).

First, we observed the extent of the linear amplification of rbCLCA products by varying the repeat time of PCR in rat cerebrum and cerebellum. As shown in Fig. 4A, the linearly amplified rbCLCA products are observed up to 50 repeats in both organs, whereas β-actin amplification products were saturated at 41 repeats. We

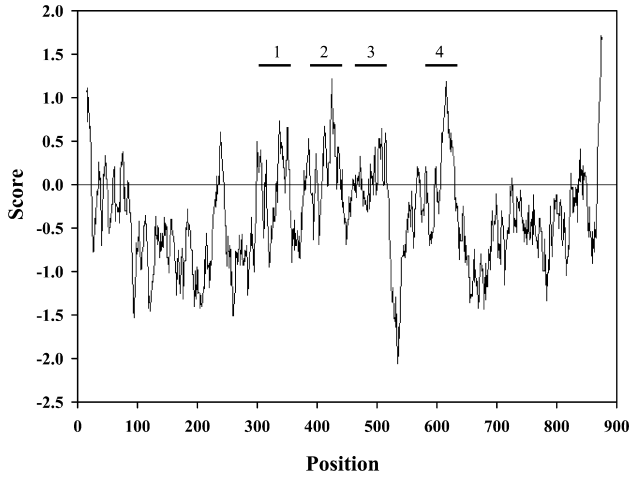

Fig. 3. Hydrophobicity plot of the rbCLCA4 amino acid sequence (Kyte–Doolittle analysis). Hydrophobic domains are given as positive values. The proposed transmembrane segments are indicated by horizontal lines, corresponding to the segments. The hydrophobicity plot is similar to that of mCLCA4.

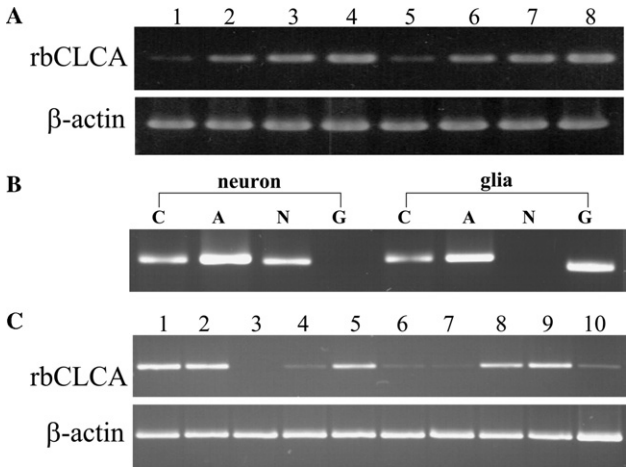

Fig. 4. Tissue distribution of rbCLCA expression in rat by RT-PCR. The first cDNA was synthesized from RNA as shown in Fig. 1. Two rounds of PCR are carried out 45 repeats to determine the specific products of rbCLCA and β-actin gene. The β-actin gene was used as internal control. Two rounds of PCR are carried out in a Peltier thermal cycler PTC-200 as described under Materials and methods. (A) The linear amplification of PCR products was observed by varying the repeat time of PCR in rat brain tissues. Upper and lower panels, lanes 1–4: 41, 44, 47, and 50 repeats in cerebrum, respectively. Lanes 5–8: 41, 44, 47, and 50 repeats in cerebellum, respectively. (B) 468 bp of rbCLCA products are observed in both the neuronal and glial single cell. C, rbCLCA (468 bp), A, β-actin as internal control (488 bp), N, neuron-specific enolase (NSE, 456 bp) as the positive control only for neuron, G, glial fibrillary acidic protein (GFAP, 420 bp) as the positive control only for glia. (C) rbCLCA products are most abundantly observed in rat brain tissues. Lanes 1–10 represent cerebrum, cerebellum, heart, lung, stomach, liver, spleen, kidney, small intestine, and large intestine, respectively.

performed single cell RT-PCR to know whether rbCLCA has a selective expression in neuron or glia. As shown in Fig. 4B, both cells showed almost same extent of rbCLCA expression, indicating that rbCLCA is not limited to only neuron or glia. As a next step, to examine the tissue variation of rbCLCA expression, we also performed the 45 repeats of RT-PCR in various organs such as cerebrum, cerebellum, heart, lung, stomach, liver, spleen, kidney, small intestine, and large intestine. The specific bands of the expected size in 468 bp of rbCLCA and 488 bp of β-actin were clearly observed (Fig. 4C). The highest expression was observed in brain cerebrum and cerebellum and the order of sequence of CLCA expression was cerebrum = cerebellum > small intestine > stomach = kidney > large intestine > lung > liver > spleen > heart.

The functional expression of the rbCLCA as anion channel was investigated by transfection into HEK293 cells with the corresponding cDNAs. In current–voltage relationship, HEK293 cells showed a slightly outwardly rectifying current with voltage-dependent manner that was significantly higher than that in mock control cells (Fig. 5). Thus, the depolarization to 80 mV at a holding potential of −70 mV induced a large outward current

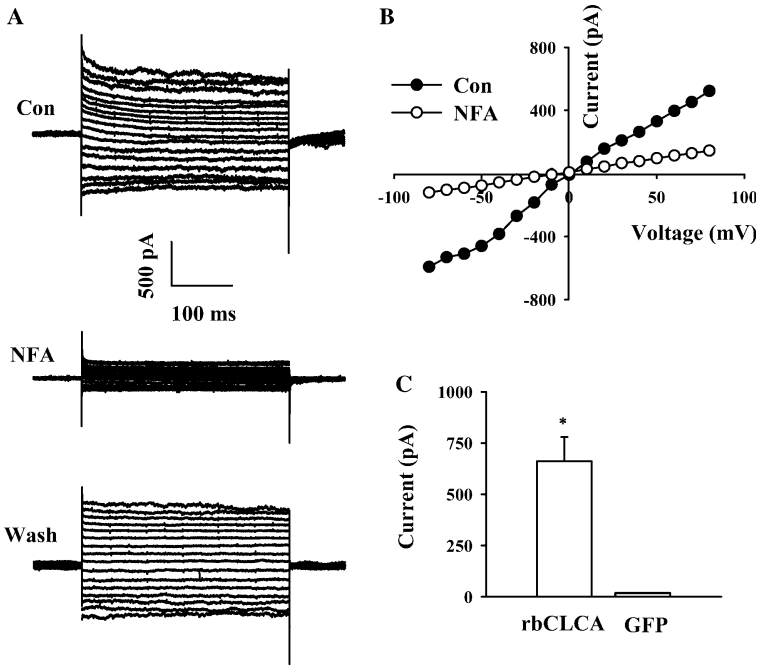

Fig. 5. Ca^{2+} activated whole-cell currents and current–voltage relationships from HEK293 cells transiently transfected with rbCLCA cDNA. rbCLCA whole-cell currents were activated and measured in response to 21 s steps to variable test voltages by 4.5 μM free Ca^{2+}. Voltage steps were in 10 mV steps from −80 to 80 mV starting from a holding potential of −70 mV. (A) Top: the control (Con) current in rbCLCA transfected HEK293 cell. Middle: after 5 min treatment with 300 μM niflumic acid (NFA), bottom: after wash for 5 min. (B) The current–voltage relationship obtained before or during treatment with niflumic acid. Each point is mean ± SEM of three experiments. (C) Mean current amplitudes obtained from the depolarization to 80 mV at a holding potential of −70 mV in EGFP + rbCLCA or EGFP alone transiently transfected HEK293 cells. EGFP + rbCLCA transfected cells ($n = 10$) showed significantly larger holding current than EGFP alone ($n = 10$) ($p < 0.0001$, unpaired t test).

and the mean current amplitude was -660 ± 118.4 nA ($n = 10$, three different batch of cells) and -18.17 ± 0.74 nA ($n = 10$) for rbCLCA and mock-transfected cell, respectively ($p < 0.0001$, compared to mock-transfected cells) (Fig. 5C). In rbCLCA-transfected cells, the reversal potential of the membrane currents was close to 0 mV, which is well consistent with an anion-selective channel. We also used a chloride channel blocker, niflumic acid, which is a strong blocker of the endogenous Ca^{2+}-activated Cl^- current in *Xenopus* oocytes [23]. In the presence of 100 μM niflumic acid, the Cl^- current induced by rbCLCA transfection was slightly blocked (data not shown) but at 300 μM niflumic acid almost blocked Cl^- current induced by rbCLCA cDNA transfection (Fig. 5).

It is known that there are at least three different types of Cl^- channels using electrophysiological studies. The first type of Cl^- channel includes the superfamily of ligand-gated chloride channels (e.g., the glycine and $GABA_A$ receptors). These chloride channels typically have four transmembrane domains and require assembly to pentamers for pharmacological or physiological functions. The second type of chloride channel comprises the ClC gene family. ClC channels may have 12 transmembrane domains and predominantly function as voltage-dependent channels. Their tissue expression varies greatly from one ClC member to another, with mutations in these genes accounting for diverse chloride conductance disorders. The third family of chloride channels is CLCAs [24]. Although the first two types of anion channels are relatively well understood with respect to their molecular identity, channel properties, and physiological roles, the CLCAs are still unresolved and controversial because of lacks of selective and specific CLCA antagonists and molecular target of CLCAs [25]. However, the characteristic hallmark of CLCA is the activation by cytosolic Ca^{2+}, which is experimentally can be induced by stimulating cells with Ca^{2+}-mobilizing agents, by Ca^{2+} ionophores such as ionomycin, by loading cells with Ca^{2+}-containing pipette solutions.

In the present study, we found that a cDNA (rbCLCA) that we have cloned from rat brain is one of the subtypes of CLCAs. Especially, rbCLCA shows a large homology with mCLCA4 (79.1% homology between rbCLCA and mCLCA4 as shown in Fig. 2). We found through hydropathy analysis that rbCLCA protein has four major potential transmembrane-spanning domains and that rbCLCA also has several motif sites for myristoylation, glycosylation, and phosphorylation by PKC, cAMP- and cGMP-dependent protein kinase, tyrosine kinase, and casein kinase II (Fig. 2). We could also observe that rbCLCA cloned from rat brain is

expressed in both neuron and glia and further found that rbCLCA is widely expressed in cerebrum, cerebellum, small intestine, stomach, and kidney, and less expressed in large intestine, lung, liver, and spleen. Interestingly, we could not observe the expression of rbCLCA in heart, although heart has its endogenous CLCAs [1,2] (Fig. 4C).

We also successfully expressed the functional rbCLCA in HEK293 cells with two evidences. As a first evidence, we showed that in cells transfected with cDNAs the loading with Ca^{2+}-containing pipette solutions exhibited a large outwardly rectifying current with reversal potential at near 0 mV, which indicates that this channel required intracellular Ca^{2+} elevation for rbCLCA activation and is anion-selective current. However, we could not observe such a current in mock-transfected cells with only EGFP vector. The second evidence is that the current evoked by loading with Ca^{2+}-containing pipette solutions was blocked by niflumic acid, a Cl^- channel blocker. Interestingly, we could observe a slight inhibition of Cl^- current at dose of 100 μM niflumic acid (data not shown) but at 300 μM niflumic acid the Cl^- current was completely blocked (Fig. 5). These results suggest two possibilities in niflumic acid-induced Cl^- channel regulation. One possibility is that the cloned rbCLCA in the present study might be less sensitive to niflumic acid compared with other types of CLCAs. Similar to our results, Cunningham et al. [17] showed that epithelial chloride channel, which was cloned from bovine trachea and expressed in COS-7 cells and *Xenopus* oocytes, was sensitive to 100 μM DIDS but not 100 μM niflumic acid. The other possibility is that niflumic acid could be permeable to membrane and block rbCLCA at the intracellular side. Qu and Hartzell [26] also demonstrated that niflumic acid applied to the cytoplasmic face of inside–out patches also blocked both inward and outward current. Therefore, we could presume that niflumic acid might act at the intracellular side and might require a higher concentration to access the intracellular side.

In summary, we have identified a clone from rat cerebrum that encodes a protein that behaves as a Ca^{2+}-activated Cl^- channel when expressed in mammalian HEK293 cells. Interestingly, this newly identified channel shares a large homology with mCLCA4 (79.1%), which is identified by Elble et al. [18]. Our current data identify rbCLCA as a candidate for Ca^{2+}-activated Cl^- channel in rat brain. Further studies will be required for the elucidation of physiological or pharmacological roles of this channel in brain.

Acknowledgments

This research was supported by grants from the Neurobiology Research Program and Brain Research Center of the 21st Century Frontier Research Program from the Korea Ministry of Science and Technology (M103KV010008 05K2201 00830).

References

[1] R.D. Harvey, J.R. Hume, Autonomic regulation of a chloride current in heart, Science 244 (1989) 983–985.
[2] A.C. Zygmunt, W.R. Gibbons, Calcium-activated chloride current in rabbit ventricular myocytes, Circ. Res. 68 (1991) 424–437.
[3] W.H. Cliff, R.A. Frizzell, Separate Cl^- conductances activated by cAMP and Ca^{2+} in Cl(−)-secreting epithelial cells, Proc. Natl. Acad. Sci. USA 87 (1990) 4956–4960.
[4] M. Hallani, J.W. Lynch, P.H. Barry, Characterization of calcium-activated chloride channels in patches excised from the dendritic knob of mammalian olfactory receptor neurons, J. Membr. Biol. 161 (1998) 163–171.
[5] C.D. Lascola, R.P. Kraig, Whole-cell chloride currents in rat astrocytes accompany changes in cell morphology, J. Neurosci. 16 (1996) 2532–2545.
[6] L.H. Clapp, J.L. Turner, R.Z. Kozlowski, Ca^{2+}-activated Cl^- currents in pulmonary arterial myocytes, Am. J. Physiol. 270 (1996) H1577–H1584.
[7] Q. Wang, R.C. Hogg, W.A. Large, Properties of spontaneous inward currents recorded in smooth muscle cells isolated from the rabbit portal vein, J. Physiol. (Lond.) 451 (1992) 525–537.
[8] M.G. Evans, A. Marty, Calcium-dependent chloride currents in isolated cells from rat lacrimal glands, J. Physiol. (Lond.) 378 (1986) 437–460.
[9] L.A. Jaffe, N.L. Cross, Electrical regulation of sperm-egg fusion, Ann. Rev. Physiol. 48 (1986) 191–200.
[10] H. Atherton, J. Mesher, C.T. Poll, H. Danahay, Preliminary pharmacological characterization of an interleukin-13-enhanced calcium-activated chloride conductance in the human airway epithelium, Naunyn Schmiedebergs Arch. Pharmacol. 367 (2003) 214–217.
[11] M. Toda, M.K. Tulic, R.C. Levitt, Q. Hamid, A calcium-activated chloride channel (HCLCA1) is strongly related to IL-9 expression and mucus production in bronchial epithelium of patients with asthma, J. Allergy Clin. Immunol. 109 (2002) 246–250.
[12] M. Hoshino, S. Morita, H. Iwashita, Y. Sagiya, T. Nagi, A. Nakanishi, Y. Ashida, O. Nishimura, Y. Fujisawa, M. Fujino, Increased expression of the human Ca^{2+}-activated Cl^- channel 1 (CaCC1) gene in the asthmatic airway, Am. J. Respir. Crit. Care Med. 165 (2002) 1132–1136.
[13] S.A. Bustin, S.R. Li, S. Dorudi, Expression of the Ca^{2+}-activated chloride channel genes CLCA1 and CLCA2 is downregulated in human colorectal cancer, DNA Cell Biol. 20 (2001) 331–338.
[14] R.C. Elble, B.U. Pauli, Tumor suppression by a proapoptotic calcium-activated chloride channel in mammary epithelium, J. Biol. Chem. 276 (2001) 40510–40517.
[15] A.D. Gruber, B.U. Pauli, Tumorigenicity of human breast cancer is associated with loss of the Ca^{2+}-activated chloride channel CLCA2, Cancer Res. 59 (1999) 5488–5491.
[16] C.H. Hartzell, I. Putzier, J. Arreola, Calcium-activated chloride channels, Annu. Rev. Physiol. 67 (2005) 719–758.
[17] S.A. Cunningham, M.S. Awayda, J.K. Bubien, I.I. Ismailov, M. Pia Arrate, B.K. Berdiev, D.J. Benos, C.M. Fuller, Cloning of epithelial chloride channel from bovine trachea, J. Biol. Chem. 270 (1995) 31016–31026.
[18] R.C. Elble, G. Ji, K. Nehrke, J. DeBiasio, P.D. Kingsley, M.I. Kotlikoff, B.U. Pauli, Molecular and functional charac-

terization of a murine calcium-activated chloride channel expressed in smooth muscle, J. Biol. Chem. 277 (2002) 18586–18591.

[19] R. Gandhi, B.C. Elble, A.D. Gruber, K.D. Schreur, H.L. Ji, C.M. Fuller, B.U. Pauli, Molecular and functional characterization of a calcium-sensitive chloride channel from mouse lung, J. Biol. Chem. 273 (1998) 32096–32101.

[20] A.D. Gruber, R.C. Elble, H.L. Ji, K.D. Scheur, C.M. Fuller, B.U. Pauli, Genomic cloning, molecular characterization, and functional analysis of human CLCA1, the first human member of the family of Ca^{2+}-activated Cl^- channel proteins, Genomics 54 (1998) 200–214.

[21] A.D. Gruber, K.D. Scheur, H.L. Ji, C.M. Fuller, B.U. Pauli, Molecular cloning and transmembrane structure of hCLCA2 from human lung, trachea, and mammary gland, Am. J. Physiol. 276 (1999) C1261–C1270.

[22] N. Akaike, A.J. Moorhouse, Techniques: applications of the nerve-bouton preparation in neuropharmacology, Trends Pharmacol. Sci. 24 (2003) 44–47.

[23] S. Choi, S.H. Rho, S.Y. Jung, S.C. Kim, C.S. Park, S.Y. Nah, A novel activation of Ca^{2+}-activated Cl^- channel in *Xenopus* oocytes by ginseng saponins: evidence for the involvement of phospholipase C and intracellular Ca^{2+} mobilization, Br. J. Pharmacol. 132 (2001) 641–648.

[24] T.J. Jentsch, V. Stein, F. Weinreich, A.A. Zdebik, Molecular structure and physiological function of chloride channels, Physiol. Rev. 82 (2002) 503–568.

[25] J. Eggermont, Calcium-activated chloride channels: unknown or unloved? Proc. Am. Thorac. Soc. 1 (2004) 22–27.

[26] Z. Qu, H.C. Hartzell, Functional geometry of the permeation pathway of Ca^{2+}-activated Cl^- channels inferred from analysis of voltage-dependent block, J. Biol. Chem. 276 (2001) 18423–18429.